Geometric Neural Diffusion Processes

Vincent Dutordoir

15th September 2023

Alan Turing Institute
Uncertainty Quantification for Generative Modelling

UNIVERSITY OF CAMBRIDGE

Papers of Reference and Collaborators

Neural Diffusion Processes. ICML 2023.

Vincent Dutordoir

Alan Saul

Zoubin Ghahramani

Fergus Simpson

Geometric Neural Diffusion Processes. Under submission.

Émile Mathieu*

Vincent Dutordoir*

Michael Hutchinson*

Valentin De Bortoli

Yee Whye Teh

Richard E. Turner

Deep generative modelling

Motivating examples

Molecular conformation generation (Xu et al., 2022)

Motif-Scaffolding (Trippe et al., 2022)

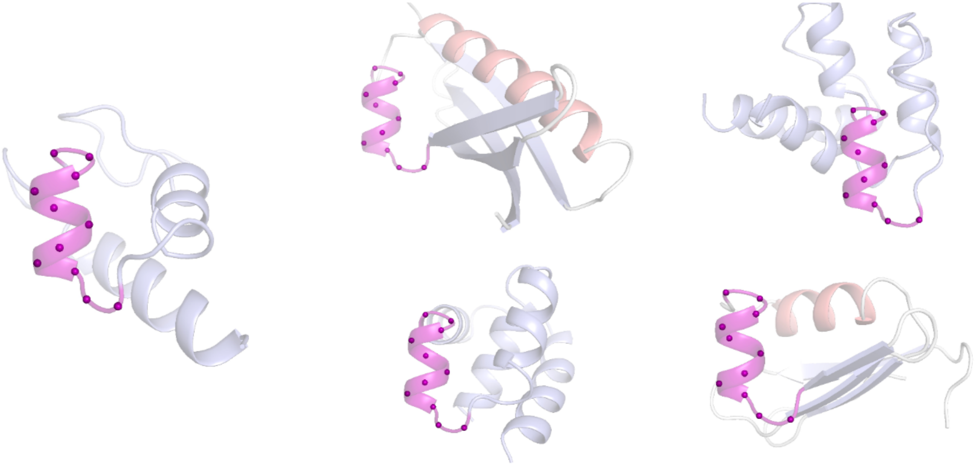

Motivating examples (Cont'd)

Probabilistic near future (nowcasting) prediction of precipitation (Ravuri et al., 2021)

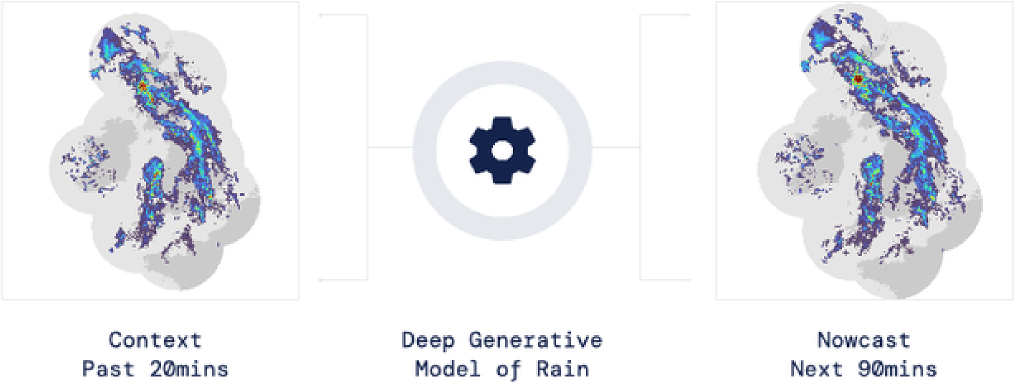

What is generative modelling?

Given $x_1, x_2, \ldots, x_n \sim p(x)$

How to model the (unknown) density $p(x)$ and sample from it?

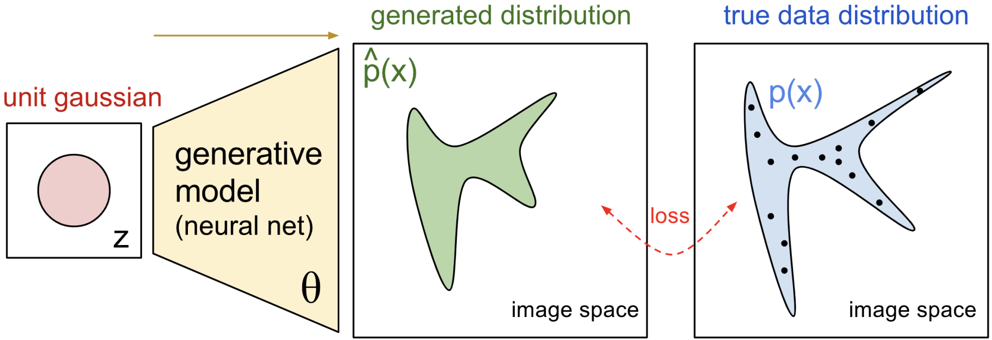

Deep generative models

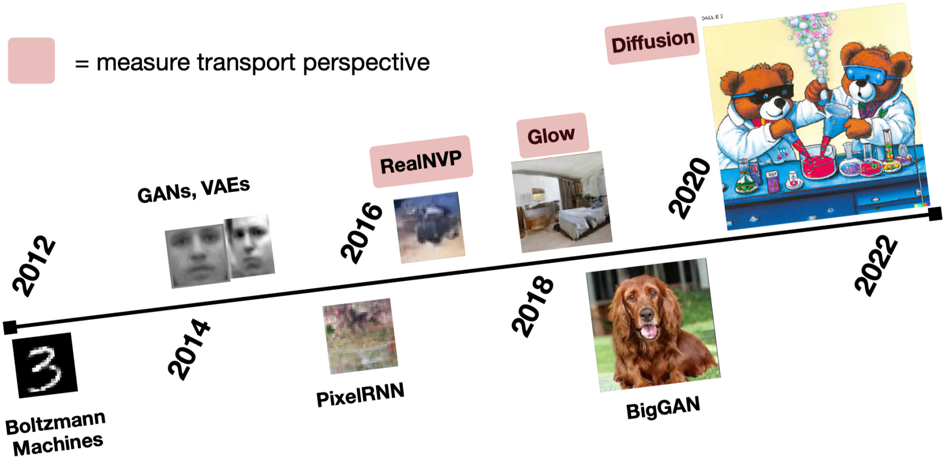

Figure 1: (Albergo and Vanden-Eijnden, 2022)

Continuous diffusion models

Principles of continuous diffusion models

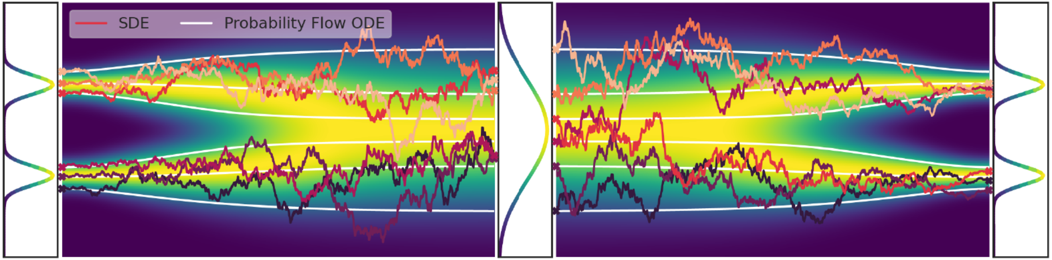

Figure 2: (Song et al., 2021)

- Idea: Destruct data with *continuous* series of noise.
- Do this by constructing an **SDE** forward noising process $(\mathbf{Y}_t)_{t\in[0,T]}$.
- Have this noising converge to a **known distribution**.
- **Invert** this SDE noising process to get $(\bar{\mathbf{Y}}_t)_{t\in[0,T]} = (\mathbf{Y}_{T-t})_{t\in[0,T]}$.

Continuous noising processes

The **Forward process** progressively perturbs the data following a SDE

$$\mathrm{d}\mathbf{Y}_t = b(t, \mathbf{Y}_t)\,\mathrm{d}t + \sigma(t, \mathbf{Y}_t)\,\mathrm{d}\mathbf{B}_t \tag{1}$$

characterised by a drift b and difffusion σ. $\mathrm{d}\mathbf{B}_t$ is Brownian motion (think of it conceptually as $\mathrm{d}\mathbf{B}_t/\mathrm{d}t \sim \mathcal{N}(0, \mathrm{d}t)$.

Continuous noising processes

The **Forward process** progressively perturbs the data following a SDE

$$\mathrm{d}\mathbf{Y}_t = b(t, \mathbf{Y}_t)\,\mathrm{d}t + \sigma(t, \mathbf{Y}_t)\,\mathrm{d}\mathbf{B}_t \tag{1}$$

characterised by a drift b and difffusion σ. $\mathrm{d}\mathbf{B}_t$ is Brownian motion (think of it conceptually as $\mathrm{d}\mathbf{B}_t/\mathrm{d}t \sim \mathcal{N}(0, \mathrm{d}t)$.

Euler–Maruyama discretisation with time step $\Delta_T \ll 1$ yields a Markov kernel:

$$p(\boldsymbol{Y}_{n+1}|\boldsymbol{Y}_n) \approx \mathcal{N}(\boldsymbol{Y}_{n+1}|\boldsymbol{Y}_n + \Delta_T\, b(t_n, \boldsymbol{Y}_n)\,, \Delta_T\, \sigma^2(t_n, \boldsymbol{Y}_n)\,\mathbf{I}).$$

where $t_n = n\Delta T$.

Example: Ornstein–Uhlenbeck process on $\mathbb{R}^2$

Let the data $\mathbf{Y}_0 \in \mathbb{R}^2$ be distributed according to a *known* 2D Gaussian with a correlation coefficient $\rho \approx 1$.

We specify the drift to be linear and the diffusion coefficient to be constant

$$\mathrm{d}\mathbf{Y}_t = -\mathbf{Y}_t \,\mathrm{d}t + \sqrt{2}\,\mathrm{d}\mathbf{B}_t. \tag{2}$$

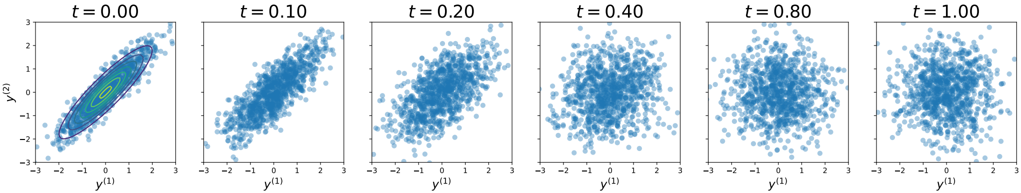

Figure 3: Forward OU process on 2D data.

Example: Ornstein–Uhlenbeck process on $\mathbb{R}^2$

Let the data $\mathbf{Y}_0 \in \mathbb{R}^2$ be distributed according to a *known* 2D Gaussian with a correlation coefficient $\rho \approx 1$.

We specify the drift to be linear and the diffusion coefficient to be constant

$$\mathrm{d}\mathbf{Y}_t = -\mathbf{Y}_t \, \mathrm{d}t + \sqrt{2} \, \mathrm{d}\mathbf{B}_t. \tag{2}$$

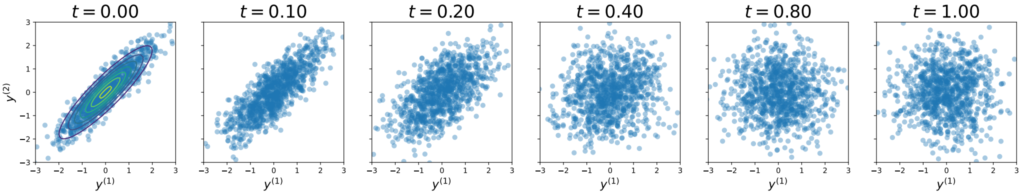

Figure 3: Forward OU process on 2D data.

Continuous score-based models: Time reversal process

Theorem 1: (Cattiaux et al., 2021; Haussmann and Pardoux, 1986)

The time-reversed process $(\bar{\mathbf{Y}}_t)_{t\geq 0} = (\mathbf{Y}_{T-t})_{t\in[0,T]}$, with forward process $\mathrm{d}\mathbf{Y}_t = b(t, \mathbf{Y}_t)\,\mathrm{d}t + \sigma(t)\,\mathrm{d}\mathbf{B}_t$, also satisfies an SDE given by

$$\mathrm{d}\bar{\mathbf{Y}}_t = \left[-b(T-t, \bar{\mathbf{Y}}_t) + \sigma(T-t)^2\,\nabla \log p_{T-t}(\bar{\mathbf{Y}}_t)\right]\mathrm{d}t + \sigma(T-t)\,\mathrm{d}\mathbf{B}_t,$$

assuming $\bar{\mathbf{Y}}_0$ is distributed the same as $\mathbf{Y}_T$.

Continuous score-based models: Time reversal process

Theorem 2: (Cattiaux et al., 2021; Haussmann and Pardoux, 1986)

The time-reversed process $(\bar{\mathbf{Y}}_t)_{t\geq 0} = (\mathbf{Y}_{T-t})_{t\in[0,T]}$, with forward process $\mathrm{d}\mathbf{Y}_t = b(t, \mathbf{Y}_t)\,\mathrm{d}t + \sigma(t)\,\mathrm{d}\mathbf{B}_t$, also satisfies an SDE given by

$$\mathrm{d}\bar{\mathbf{Y}}_t = \left[-b(T-t, \bar{\mathbf{Y}}_t) + \sigma(T-t)^2\,\nabla \log p_{T-t}(\bar{\mathbf{Y}}_t)\right]\mathrm{d}t + \sigma(T-t)\,\mathrm{d}\mathbf{B}_t,$$

assuming $\bar{\mathbf{Y}}_0$ is distributed the same as $\mathbf{Y}_T$.

Challenges:

1. We do not have access to $\mathbf{Y}_T \Rightarrow$ Approximate as $\mathbf{Y}_T \approx \mathbf{Y}_\infty$!
2. The Stein score $\nabla \log p_t$ is intractable (requires solving Fokker-Planck...) $\Rightarrow$ learn it!
3. Cannot solve the SDE exactly $\Rightarrow$ discretise!

Learning the score (Hyvärinen, 2005; Vincent, 2011; Song et al., 2021)

- The Stein score $\nabla \log p_t = \nabla \log \int p_{data}(\mathbf{Y}_0) p_{t|0}(\mathbf{Y}_t \mid \mathbf{Y}_0) \mathrm{d}\mathbf{Y}_0$ is intractable.
- However, it can be shown that the score is the minimiser of regression objective

$$\nabla_{\mathbf{Y}_t} \log p_t(\mathbf{Y}_t) = \arg\min_{s \in \mathcal{S}} \mathbb{E}\left[\|\mathbf{s}(t, \mathbf{Y}_t) - \nabla_{\mathbf{Y}_t} \log p_{t|0}(\mathbf{Y}_t|\mathbf{Y}_0)\|^2 \right], \quad (3)$$

  where the expectation is taken over the joint $(t, \mathbf{Y}_0, \mathbf{Y}_t)$.
- We have access to the conditional forward density $p_{t|0}$ in closed form for OU processes.
- This readily gives a loss to train a neural network $\mathbf{s}_\theta : [0, T] \times \mathbb{R}^d \to \mathbb{R}^d$ parameterisation of the score

$$\mathcal{L}(\theta) = \mathbb{E}[\lambda(t) \| \mathrm{s}_\theta(t, \mathbf{Y}_t) - \nabla \log p_t(\mathbf{Y}_t|\mathbf{Y}_0)\|^2]. \quad (4)$$

Sampling from the reverse process in practice

The (true) reverse process is given by

$$\mathrm{d}\bar{\mathbf{Y}}_t = \left[-b(T-t, \bar{\mathbf{Y}}_t) + \sigma(T-t)^2 \nabla \log p_{T-t}(\bar{\mathbf{Y}}_t) \right] \mathrm{d}t + \sigma(T-t)\, \mathrm{d}\mathbf{B}_t.$$

We make the following approximations

1. Initialise $\bar{\mathbf{Y}}_0 \sim \mathcal{N}(\mathbf{0}, \boldsymbol{I})$ which approximates $p(\mathbf{Y}_T)$.
2. Use score approximation $\nabla \log p_{T-t}(\bar{\mathbf{Y}}_t) = \boldsymbol{s}_\theta(T-t, \bar{\mathbf{Y}}_t)$.
3. Discretise SDE using Euler–Maruyama method

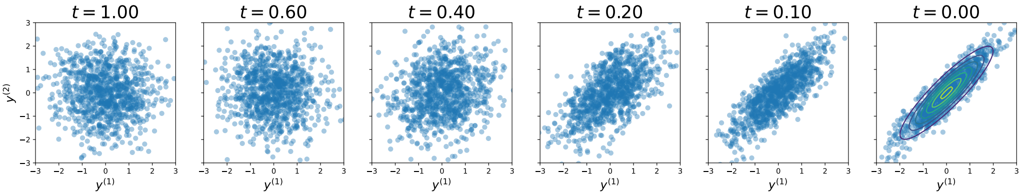

Improved sampling using Langevin dynamics

- Euler-Maruyama method introduces discretisation errors.
- Song et al. 2021 suggest to use Langevin dymanics to correct each reverse step.

Improved sampling using Langevin dynamics

- Euler-Maruyama method introduces discretisation errors.
- Song et al. 2021 suggest to use Langevin dymanics to correct each reverse step.

Langevin dynamics:

$$\mathrm{d}\mathbf{Y}_t = \nabla_{\mathbf{Y}_t} \log p(\mathbf{Y}_t)\,\mathrm{d}t + \sqrt{2}\,\mathrm{d}\mathbf{B}_t, \tag{5}$$

As $t \to \infty$, the dynamics converges towards the distribution $p(\cdot)$.

Improved sampling using Langevin dynamics

- Euler-Maruyama method introduces discretisation errors.
- Song et al. 2021 suggest to use Langevin dymanics to correct each reverse step.

Langevin dynamics:

$$\mathrm{d}\mathbf{Y}_t = \nabla_{\mathbf{Y}_t} \log p(\mathbf{Y}_t)\, \mathrm{d}t + \sqrt{2}\, \mathrm{d}\mathbf{B}_t, \tag{5}$$

As $t \to \infty$, the dynamics converges towards the distribution $p(\cdot)$.

Predictor-Corrector sampling

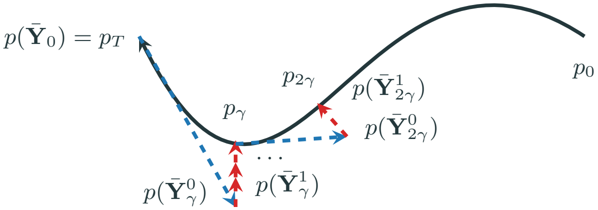

Credits to Valentin De Bortoli for graphic.

Recap: Continuous diffusion models

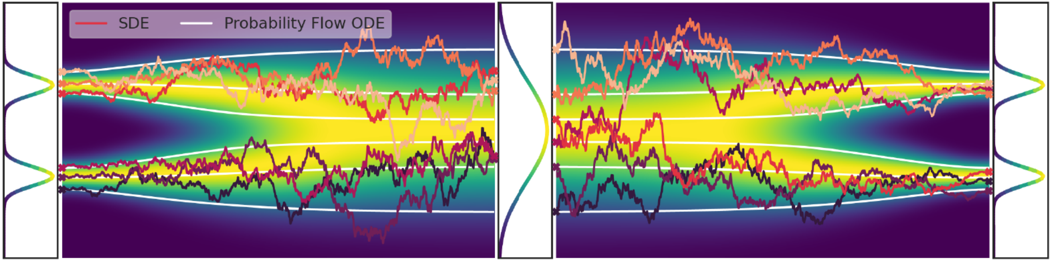

- Continuously **noise** data samples with forward SDE
- Aim: time-reversal of this process $\Rightarrow$ **denoising** process

Motivation Geometric Neural Diffusion Processes

Goal

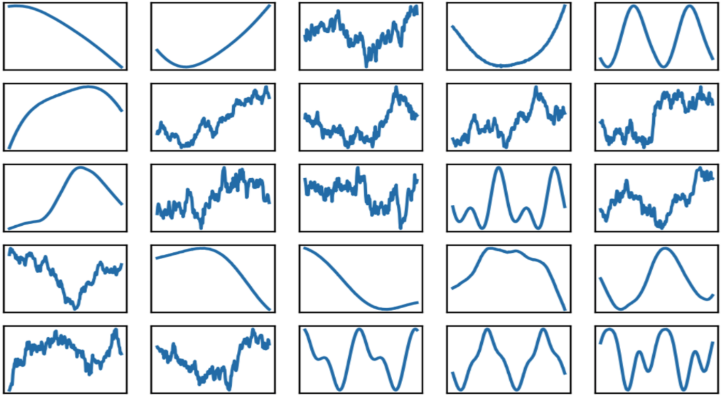

Goal

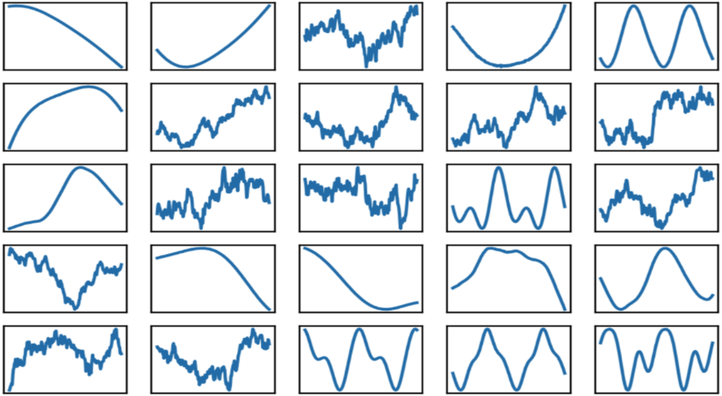

Why

- Many physical and natural phenomena are better characterised as functions.
- Meta-learn and treat limited data as originating from a function

Feature Fields: $f : \mathcal{X} \to \mathbb{R}^d$

- Mathematical framework for modelling natural phenomena.
- Examples: Temperature $f : \mathcal{X} \to \mathbb{R}$, and wind direction on globe $f : \mathcal{S}^2 \to T\mathcal{S}^2$.

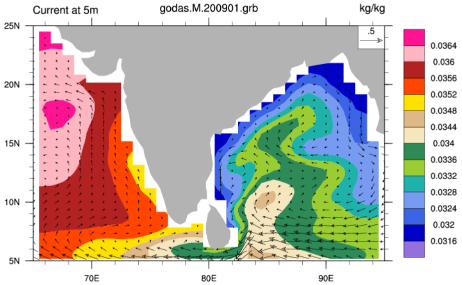

(a) Temperature map and wind vector fields.

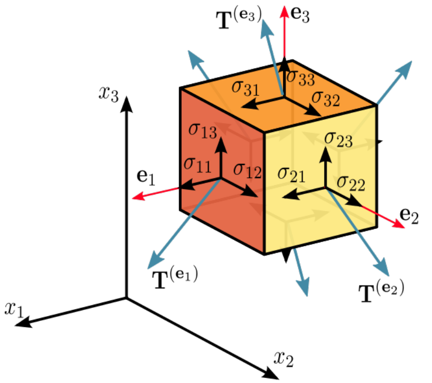

(b) 3D stress tensor (type-2) diagram.

Prior invariances

Encode invariances w.r.t. group transformations. For a group G, we want $\forall g \in G$

$$p(f) = p(g \cdot f) \quad \text{with} \quad g \cdot f = \rho(g) f(g^{-1} x).$$

Prior invariances

Encode invariances w.r.t. group transformations. For a group G, we want $\forall g \in G$

$$p(f) = p(g \cdot f) \quad \text{with} \quad g \cdot f = \rho(g) f(g^{-1} x).$$

Examples translation invariance (stationarity) and rotational invariance.

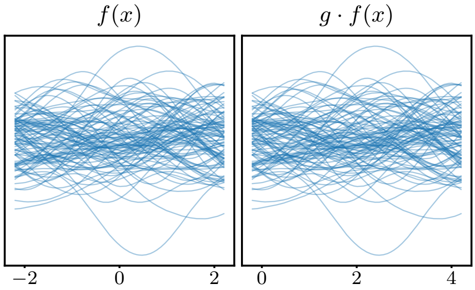

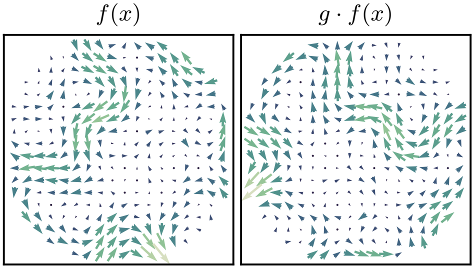

Conditional process

- Interested in the conditional process given a set of observations $\mathcal{C} = \{(x_n, y_n)\}_{n=1}$.
- If the prior is G-invariant, then the conditional is G-equivariant:

$$p(f \mid \mathcal{C}) = p(g \cdot f | g \cdot \mathcal{C}) \quad \text{where} \quad g \cdot \mathcal{C} = \{(g \cdot x_n, \rho(g) y_n)\}.$$

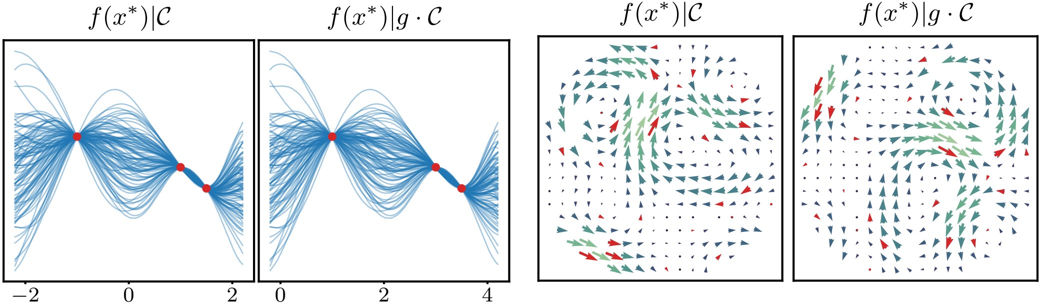

Diffusion on Function Spaces

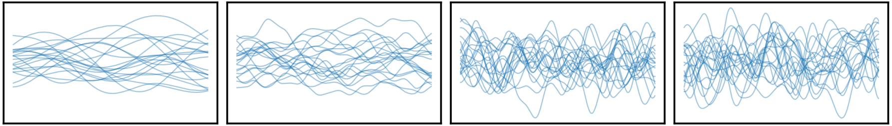

We construct the forward **noising process** $(\mathbf{Y}_t(x))_{t\geq 0} \triangleq (\mathbf{Y}_t(x^1), \ldots, \mathbf{Y}_t(x^n))_{t\geq 0}$ defined by the multivariate SDE (multivariate Ornstein-Uhlenbeck process)

$$\mathrm{d}\mathbf{Y}_t(x) = \frac{1}{2}\left\{m(x) - \mathbf{Y}_t(x)\right\}\beta_t \,\mathrm{d}t + \beta_t^{1/2}\mathrm{K}(x,x)^{1/2}\,\mathrm{d}\mathbf{B}_t, \tag{6}$$

where $\mathrm{K}(x,x)_{i,j} = k(x^i, x^j)$ with $k : \mathcal{X} \times \mathcal{X} \to \mathbb{R}$ a kernel and $m : \mathcal{X} \to \mathcal{Y}$.

Continuous noising process

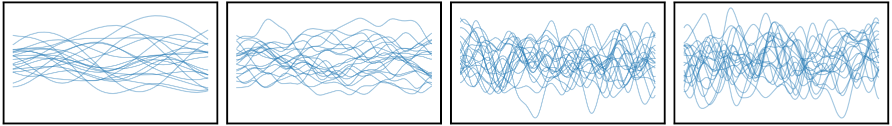

We construct the forward **noising process** $(\mathbf{Y}_t(x))_{t\geq 0} \triangleq (\mathbf{Y}_t(x^1), \dots, \mathbf{Y}_t(x^n))_{t\geq 0}$ defined by the multivariate SDE (multivariate Ornstein-Uhlenbeck process)

$$\mathrm{d}\mathbf{Y}_t(x) = \frac{1}{2}\left\{m(x) - \mathbf{Y}_t(x)\right\}\beta_t \,\mathrm{d}t + \beta_t^{1/2}\mathrm{K}(x,x)^{1/2}\,\mathrm{d}\mathbf{B}_t, \tag{6}$$

where $\mathrm{K}(x,x)_{i,j} = k(x^i, x^j)$ with $k : \mathcal{X} \times \mathcal{X} \to \mathbb{R}$ a kernel and $m : \mathcal{X} \to \mathcal{Y}$.

- $\mathbf{Y}_t(x) \to \mathrm{N}(m(x), \mathrm{K}(x,x))$ with geometric rate, for any $x \in \mathcal{X}^n$.
- $\mathbf{Y}_t \to \mathrm{GP}(m,k) \triangleq \mathbf{Y}_\infty$ (Phillips et al., 2022).

Continuous noising process

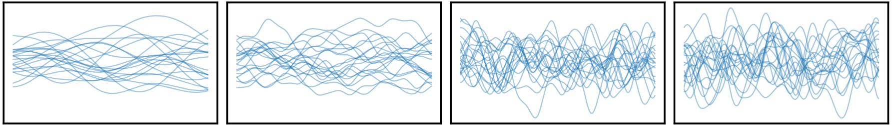

We construct the forward **noising process** $(\mathbf{Y}_t(x))_{t\geq 0} \triangleq (\mathbf{Y}_t(x^1), \dots, \mathbf{Y}_t(x^n))_{t\geq 0}$ defined by the multivariate SDE (multivariate Ornstein-Uhlenbeck process)

$$\mathrm{d}\mathbf{Y}_t(x) = \tfrac{1}{2}\{m(x) - \mathbf{Y}_t(x)\}\,\beta_t\,\mathrm{d}t + \beta_t^{1/2}\mathrm{K}(x,x)^{1/2}\,\mathrm{d}\mathbf{B}_t, \tag{6}$$

where $\mathrm{K}(x,x)_{i,j} = k(x^i, x^j)$ with $k : \mathcal{X} \times \mathcal{X} \to \mathbb{R}$ a kernel and $m : \mathcal{X} \to \mathcal{Y}$.

- $\mathbf{Y}_t(x) \to \mathrm{N}(m(x), \mathrm{K}(x,x))$ with geometric rate, for any $x \in \mathcal{X}^n$.
- $\mathbf{Y}_t \to \mathrm{GP}(m,k) \triangleq \mathbf{Y}_\infty$ (Phillips et al., 2022).
- $\mathbf{Y}_t$ interpolates between $\mathbf{Y}_0$ and $\mathbf{Y}_\infty$.
- $\mathbf{Y}_t(x)|\boldsymbol{y}_0 = \mathrm{N}(m_t(x;\boldsymbol{y}_0), \mathrm{K}_t(x,x;\boldsymbol{y}_0))$ for any $x \in \mathcal{X}^n$.

Continuous noising process

$$k(x, x') = k_{\text{rbf}}(x, x') = \sigma^2 \exp\left(\frac{\|x - x'\|^2}{2l^2}\right), \text{ with } l = 1.$$

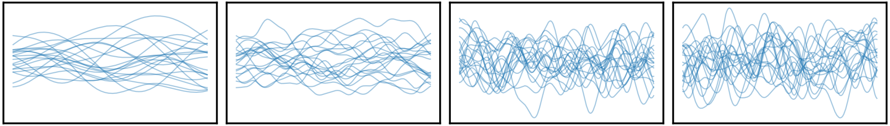

Continuous noising process

$$k(x, x') = k_{\mathrm{rbf}}(x, x') = \sigma^2 \exp\left(\frac{\|x-x'\|^2}{2l^2}\right), \text{ with } l = 1.$$

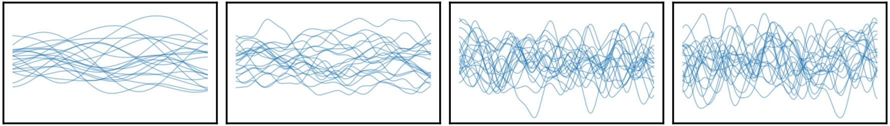

$$k(x, x') = k_{\mathrm{rbf}}(x, x'), \text{ with } l = 0.2.$$

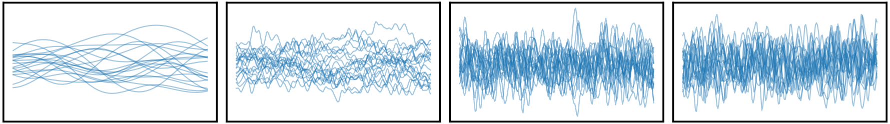

Continuous noising process

$$k(x, x') = k_{\text{rbf}}(x, x') = \sigma^2 \exp\left(\frac{\|x - x'\|^2}{2l^2}\right),$$ with $l = 1$.

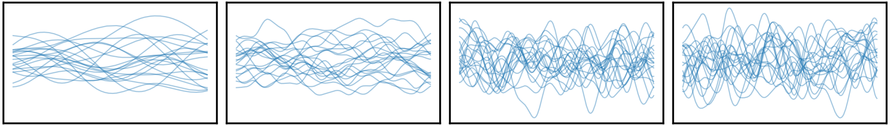

$$k(x, x') = k_{\text{rbf}}(x, x'),$$ with $l = 0.2$.

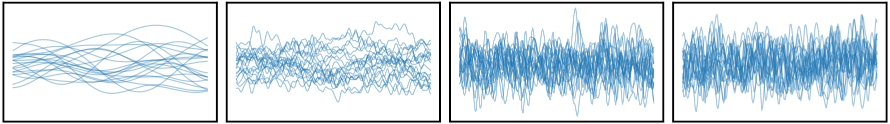

$k(x, x') = \delta_x(x')$ (The tranditional DDPM settings).

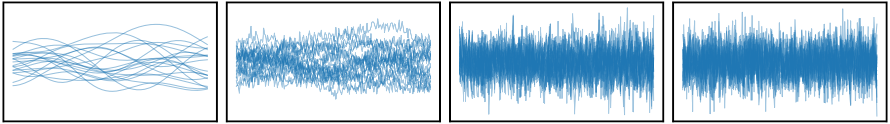

Denoising process

As before, the **time-reversal process** $(\bar{\mathbf{Y}}_t(x))_{t\geq 0}$ also satisfies an SDE given by

$$\begin{aligned} \mathrm{d}\bar{\mathbf{Y}}_t(x) = \{-\tfrac{1}{2}(m(x) - \bar{\mathbf{Y}}_t(x)) + \mathrm{K}(x,x)\nabla \log p_{T-t}(\bar{\mathbf{Y}}_t(x))\}\beta_{T-t}\mathrm{d}t \\ + \beta_{T-t}^{1/2}\mathrm{K}(x,x)^{1/2}\mathrm{d}\mathbf{B}_t, \end{aligned} \tag{7}$$

with $\bar{\mathbf{Y}}_0 \sim \mathrm{GP}(m, k)$.

Denoising process

As before, the **time-reversal process** $(\bar{\mathbf{Y}}_t(x))_{t\geq 0}$ also satisfies an SDE given by

$$\mathrm{d}\bar{\mathbf{Y}}_t(x) = \{-\tfrac{1}{2}(m(x) - \bar{\mathbf{Y}}_t(x)) + \mathrm{K}(x,x)\nabla \log p_{T-t}(\bar{\mathbf{Y}}_t(x))\}\beta_{T-t}\mathrm{d}t \\ + \beta_{T-t}^{1/2}\mathrm{K}(x,x)^{1/2}\mathrm{d}\mathbf{B}_t, \tag{7}$$

with $\bar{\mathbf{Y}}_0 \sim \mathrm{GP}(m,k)$.

To simulate the reverse process we learn the (preconditioned) score

$$\boldsymbol{s}_\theta^K(t, \bar{\mathbf{Y}}_t(x), x) \approx \mathrm{K}(x,x)\nabla \log p_{T-t}(\bar{\mathbf{Y}}_t(x)),$$

where $\boldsymbol{s}_\theta^K : \mathbb{R} \times \mathcal{Y}^m \times \mathcal{X}^m \to \mathrm{T}\mathcal{Y}^m$. We accomplish this using the score matching objective

$$\mathcal{L}(\theta) = \mathbb{E}\left[\lambda(t)\|\boldsymbol{s}_\theta^K(t, \mathbf{Y}_t(x), x) + \mathrm{K}^{1/2}\epsilon\|_2^2\right].$$

Encoding Invariances

Prior and Conditional Symmetries

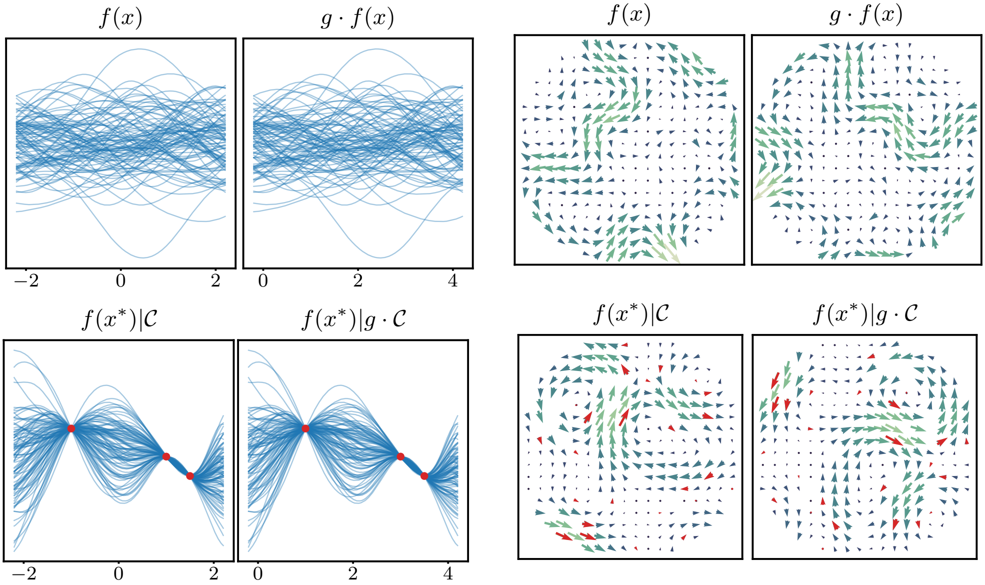

Invariant neural diffusion processes

Proposition 1: Invariant Neural Diffusion Processes

The denoising process on functions induced by

$$\mathrm{d}\bar{\mathbf{Y}}_t^{\theta}(x) = \{-\tfrac{1}{2}(m(x) - \bar{\mathbf{Y}}_t(x)) + \mathbf{s}_\theta^K(T-t, x, \bar{\mathbf{Y}}_t(x))\}\beta_{T-t}\,\mathrm{d}t + \beta_{T-t}^{1/2}\mathrm{K}(x,x)^{1/2}\,\mathrm{d}\mathbf{B}_t, \tag{8}$$

and with initial sample given by $p(\bar{\mathbf{Y}}_0) = \mathrm{GP}(m, k)$ is G-invariant if

1. m and k are both G-equivariant (i.e. G-invariant Gaussian process), and
2. the score network is G-equivariant vector field, i.e.

$$\mathbf{s}_\theta^K(t, g \cdot x, \rho(g)y) = \rho(g)\mathbf{s}_\theta(t, x, y) \text{ for all } x \in \mathcal{X}, g \in G.$$

$\mathrm{E}(d)$-invariant Gaussian processes

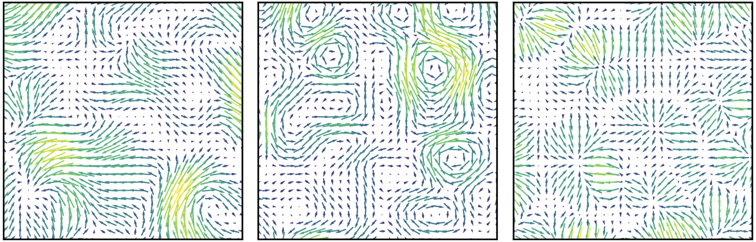

- $\mathrm{E}(d)$-equivariant means $m : \mathbb{R}^d \to \mathbb{R}^d$ are constant functions.

$\mathrm{E}(d)$-invariant Gaussian processes

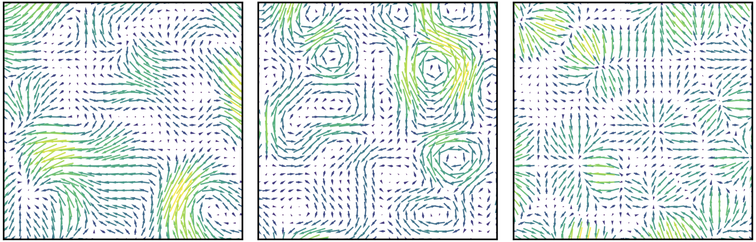

- $\mathrm{E}(d)$-equivariant means $m : \mathbb{R}^d \to \mathbb{R}^d$ are constant functions.
- $\mathrm{E}(d)$-equivariant kernels $k : \mathbb{R}^d \times \mathbb{R}^d \to \mathbb{R}^{d\times d}$ include
  - Diagonal kernels $k = k_0 \operatorname{Id}$ with k_0 invariant (Holderrieth et al., 2021).
  - $k_{\mathrm{curl}} = k_0 A$ with $A(x, x') = \operatorname{Id} - \frac{(x-x')(x-x')^\top}{l^2}$ (Macêdo and Castro, 2010).
  - $k_{\mathrm{div}} = k_0 B$ with $B(x, x') = \frac{(x-x')(x-x')^\top}{l^2} + \left(n - 1 - \frac{\|x-x'\|^2}{l^2}\right) \operatorname{Id}$.

Invariant neural diffusion processes (Cont'd)

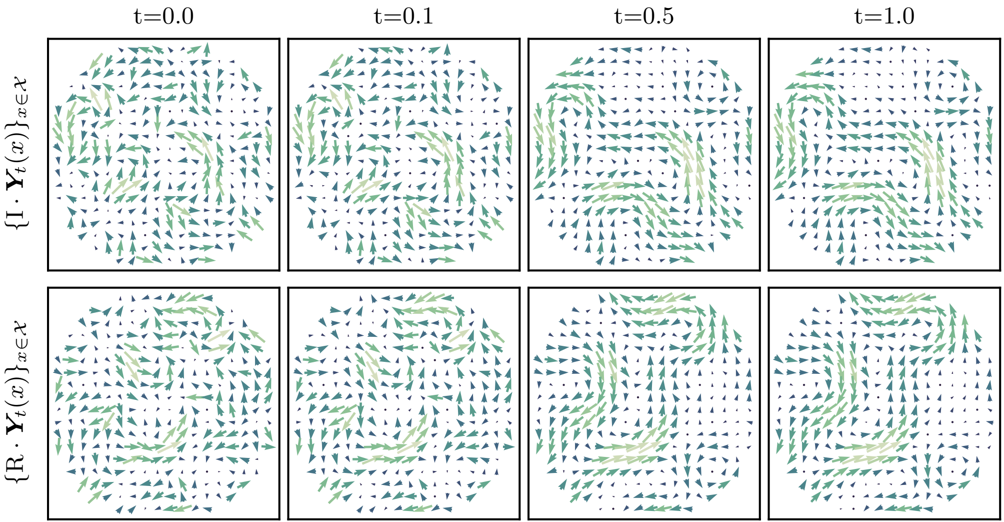

Figure 9: $(g \cdot \mathbf{Y}_t(x))_{x \in \mathcal{X}}$

Conditional processes

Conditional sampling

Conditional sampling in diffusion models

Goal: Sample from $y \sim p(\cdot \mid \mathcal{C})$ given a condition $\mathcal{C}$ Often the condition is a property (e.g., caption).

Conditional sampling in diffusion models

Goal: Sample from $y \sim p(\cdot \mid \mathcal{C})$ given a condition $\mathcal{C}$ Often the condition is a property (e.g., caption).

"a hedgehog using a calculator"

"a corgi wearing a red bowtie and a purple party hat"

"robots meditating in a vipassana retreat"

"a fall landscape with a small cottage next to a lake"

Figure 10: $p(image \mid text)$

Conditional sampling in diffusion models

Goal: Sample from $y \sim p(\cdot \mid \mathcal{C})$ given a condition $\mathcal{C}$.

Condition is a subspace of the state space: $y = (y^{(1)}, \ldots, y^{(m)})$ and $\mathcal{C} = (y^{(m+1)}, \ldots, y^{(n)})$.

Conditional sampling in diffusion models

Goal: Sample from $y \sim p(\cdot \mid \mathcal{C})$ given a condition $\mathcal{C}$.
Condition is a subspace of the state space: $y = (y^{(1)}, \ldots, y^{(m)})$ and $\mathcal{C} = (y^{(m+1)}, \ldots, y^{(n)})$.

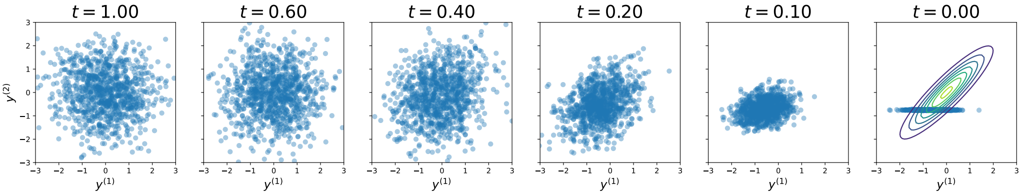

Figure 11: $p(y \mid y^{(2)} = -1)$

Conditional sampling in diffusion models

In the reverse process we need to follow the **Conditional Score**

$$\nabla \log p_t(\mathbf{Y}_t) \implies \nabla \log p_t(\mathbf{Y}_t \mid \mathcal{C})$$

Conditional sampling in diffusion models

In the reverse process we need to follow the **Conditional Score**

$$\nabla \log p_t(\mathbf{Y}_t) \implies \nabla \log p_t(\mathbf{Y}_t \mid \mathcal{C})$$

1. Amortisation / Classifier-free (Ramesh et al., 2022)
2. Classifier-guidance (Dhariwal and Nichol, 2021)
3. Replacement methods RePaint (Lugmayr et al., 2022)
4. Reconstruction guidance (Finzi et al., 2023)
5. SMC-based (Trippe et al., 2022)

Langevin Dynamics based Conditional Sampling

Focussing on the function setting, the context $\mathcal{C} = \mathbf{Y}_0^{\mathcal{C}}$

$$\begin{aligned}
\nabla_{\mathbf{Y}_t} \log p_t(\mathbf{Y}_t \mid \mathbf{Y}_0^{\mathcal{C}}) &= \nabla_{\mathbf{Y}_t} \log p_t(\mathbf{Y}_t, \mathbf{Y}_0^{\mathcal{C}}) - \nabla_{\mathbf{Y}_t} \log p_t(\mathbf{Y}_0^{\mathcal{C}}) \\
&= \nabla_{\mathbf{Y}_t} \log p_t(\mathbf{Y}_t, \mathbf{Y}_0^{\mathcal{C}})
\end{aligned}$$

Langevin Dynamics based Conditional Sampling

Focussing on the function setting, the context $\mathcal{C} = \mathbf{Y}_0^{\mathcal{C}}$

$$\begin{aligned} \nabla_{\mathbf{Y}_t} \log p_t(\mathbf{Y}_t \mid \mathbf{Y}_0^{\mathcal{C}}) &= \nabla_{\mathbf{Y}_t} \log p_t(\mathbf{Y}_t, \mathbf{Y}_0^{\mathcal{C}}) - \nabla_{\mathbf{Y}_t} \log p_t(\mathbf{Y}_0^{\mathcal{C}}) \\ &= \nabla_{\mathbf{Y}_t} \log p_t(\mathbf{Y}_t, \mathbf{Y}_0^{\mathcal{C}}) \end{aligned}$$

Predictor Use standard EM reverse process with score $s_\theta^K(t, x, [\mathbf{Y}_t, \mathbf{Y}_0^{\mathcal{C}}])$.

Corrector Correct discretisation errors using Langevin dynamics

Langevin Dynamics based Conditional Sampling

Focussing on the function setting, the context $\mathcal{C} = \mathbf{Y}_0^{\mathcal{C}}$

$$\begin{aligned}\nabla_{\mathbf{Y}_t} \log p_t(\mathbf{Y}_t \mid \mathbf{Y}_0^{\mathcal{C}}) &= \nabla_{\mathbf{Y}_t} \log p_t(\mathbf{Y}_t, \mathbf{Y}_0^{\mathcal{C}}) - \nabla_{\mathbf{Y}_t} \log p_t(\mathbf{Y}_0^{\mathcal{C}}) \\ &= \nabla_{\mathbf{Y}_t} \log p_t(\mathbf{Y}_t, \mathbf{Y}_0^{\mathcal{C}})\end{aligned}$$

Predictor Use standard EM reverse process with score $s_\theta^K(t, x, [\mathbf{Y}_t, \mathbf{Y}_0^{\mathcal{C}}])$.

Corrector Correct discretisation errors using Langevin dynamics

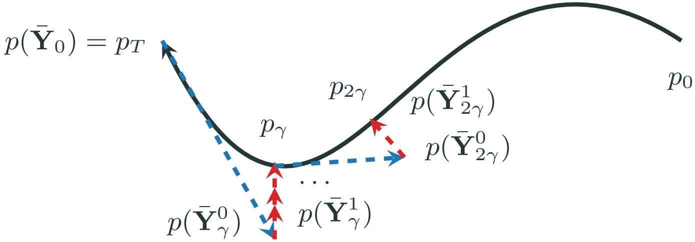

Experimental results

1D regression: Datasets

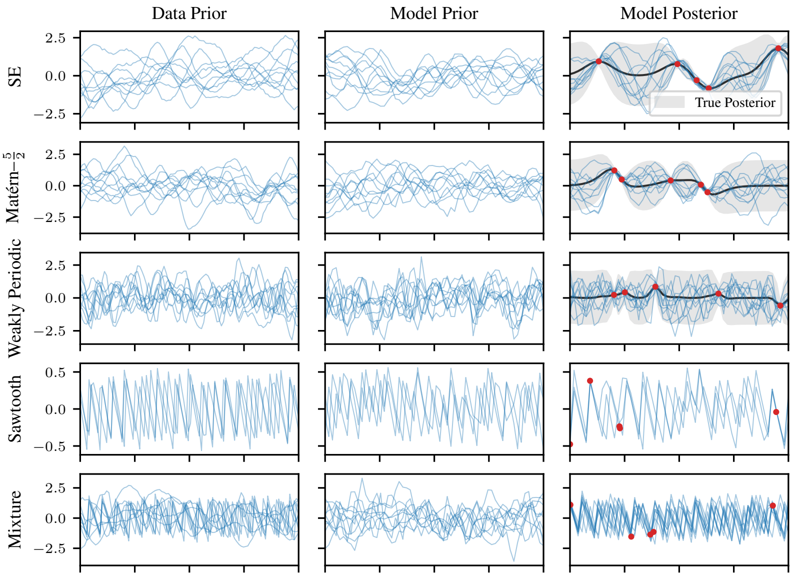

1D regression: Predictive log-likelihood (Cont'd)

Table 1: Mean test log-likelihood (TLL) (↑) ± 1 standard error estimated over 4096 test samples are reported. NP baselines from (Bruinsma et al., 2020).

		SE	Matérn($\frac{5}{2}$)	Weakly Per.	Sawtooth	Mixture
Interpolat.	GP (optimum)	$0.70{\pm}0.00$	$0.31{\pm}0.00$	$-0.32{\pm}0.00$	-	-
	T(1)−GeomNDP	$\mathbf{0.72}{\pm}0.03$	$\mathbf{0.32}{\pm}0.03$	$\mathbf{-0.38}{\pm}0.03$	$\mathbf{3.39}{\pm}0.04$	$\mathbf{0.64}{\pm}0.08$
	NDP*	$\mathbf{0.71}{\pm}0.03$	$\mathbf{0.30}{\pm}0.03$	$\mathbf{-0.37}{\pm}0.03$	$\mathbf{3.39}{\pm}0.04$	$\mathbf{0.64}{\pm}0.08$
	GNP	$\mathbf{0.70}{\pm}0.01$	$\mathbf{0.30}{\pm}0.01$	$-0.47{\pm}0.01$	$0.42{\pm}0.01$	$0.10{\pm}0.02$
	ConvNP	$-0.46{\pm}0.01$	$-0.67{\pm}0.01$	$-1.02{\pm}0.01$	$1.20{\pm}0.01$	$-0.50{\pm}0.02$
Generalisat.	GP (optimum)	$0.70{\pm}0.00$	$0.31{\pm}0.00$	$-0.32{\pm}0.00$	-	-
	T(1)−GeomNDP	$\mathbf{0.70}{\pm}0.02$	$\mathbf{0.31}{\pm}0.02$	$\mathbf{-0.38}{\pm}0.03$	$\mathbf{3.39}{\pm}0.03$	$\mathbf{0.62}{\pm}0.02$
	NDP*	*	*	*	*	*
	GNP	$\mathbf{0.69}{\pm}0.01$	$\mathbf{0.30}{\pm}0.01$	$-0.47{\pm}0.01$	$0.42{\pm}0.01$	$0.10{\pm}0.02$
	ConvNP	$-0.46{\pm}0.01$	$-0.67{\pm}0.01$	$-1.02{\pm}0.01$	$1.19{\pm}0.01$	$-0.53{\pm}0.02$

2D invariant Gaussian vector fields

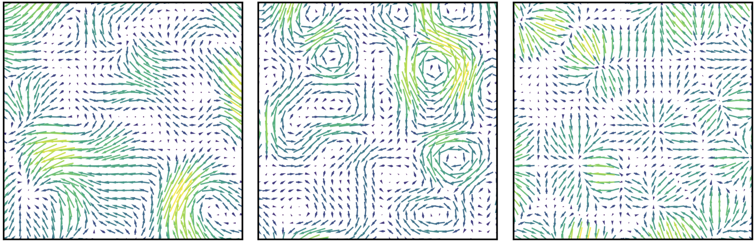

Model	SE	Curl-free	Div-free
GP	$0.56_{\pm 0.00}$	$0.66_{\pm 0.00}$	$0.66_{\pm 0.00}$
NDP*	$0.55_{\pm 0.00}$	$0.62_{\pm 0.01}$	$0.62_{\pm 0.01}$
E(2)-GeomNDP	$\mathbf{0.56_{\pm 0.01}}$	$\mathbf{0.65_{\pm 0.01}}$	$\mathbf{0.66_{\pm 0.01}}$
GP (diag.)	$-1.56_{\pm 0.00}$	$-1.47_{\pm 0.00}$	$-1.47_{\pm 0.00}$
T(2)-ConvCNP	$-1.71_{\pm 0.01}$	$-1.77_{\pm 0.01}$	$-1.76_{\pm 0.00}$
E(2)-SteerCNP	$-1.61_{\pm 0.00}$	$-1.57_{\pm 0.00}$	$-1.57_{\pm 0.01}$

2D invariant Gaussian vector fields (Cont'd)

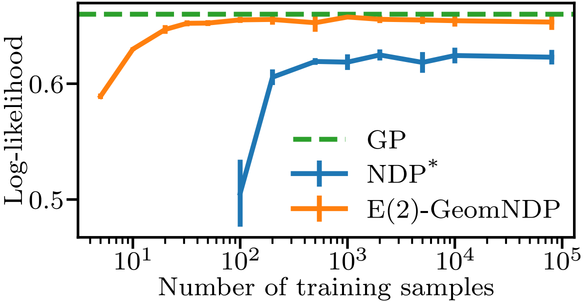

Global tropical cyclone trajectory prediction

- $f : \mathbb{R} \to \mathcal{S}^2$ with hurricane trajectory data from (Knapp et al., 2018).
- $\mathbf{Y}_t(x) = (\mathbf{Y}_t(x_1), \cdots, \mathbf{Y}_t(x_n)) \in \mathcal{M}^n$ for any $(x_1, \ldots, x_n) \in \mathbb{R}^n$
- $\mathrm{d}\mathbf{Y}_t(x_k) = \boxed{-\cancelto{0}{b(\mathbf{Y}_t(x_k))}}\,\mathrm{d}t + \boxed{\sqrt{\beta_t}}\,\mathrm{d}\mathbf{B}_t^{\mathcal{M}}$ $\forall k = 1, \ldots, n$ (Bortoli et al., 2022)
- $p(\mathbf{Y}_t(x)) \underset{t\to\infty}{\longrightarrow} \mathrm{U}(\mathcal{S}^2)^{\otimes n}$.

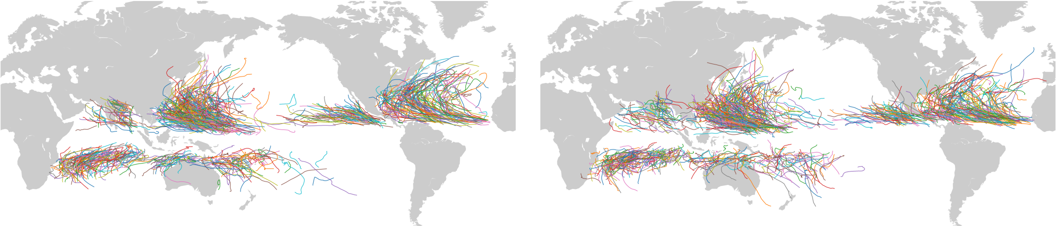

Figure 12: *Left:* 1000 samples from the training data. *Right:* 1000 samples from trained model.

Global tropical cyclone trajectory prediction (Cont'd)

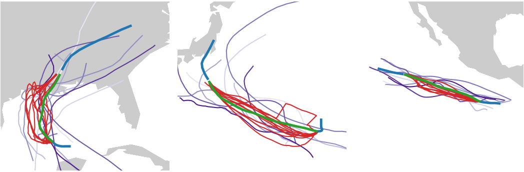

(a) Interpolation

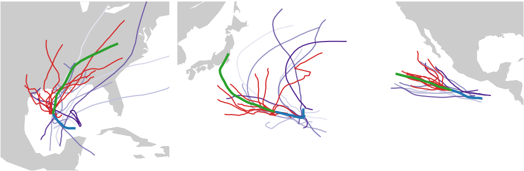

(b) Extrapolation

Model	Test data	Interpolation		Extrapolation	
	Likelihood	Likelihood	MSE (km)	Likelihood	MSE (km)
GeomNDP($\mathbb{R} \to \mathcal{S}^2$)	$\mathbf{802}_{\pm 5}$	$\mathbf{535}_{\pm 4}$	$\mathbf{162}_{\pm 6}$	$\mathbf{536}_{\pm 4}$	$\mathbf{496}_{\pm 14}$
Stereo GP ($\mathbb{R} \to \mathbb{R}^2/\{0\}$)	$393_{\pm 3}$	$266_{\pm 3}$	$2619_{\pm 13}$	$245_{\pm 2}$	$6587_{\pm 55}$
NDP ($\mathbb{R} \to \mathbb{R}^2$)	-	-	$166_{\pm 22}$	-	$769_{\pm 48}$
GP ($\mathbb{R} \to \mathbb{R}^2$)	-	-	$6852_{\pm 41}$	-	$8138_{\pm 87}$

Recap: Geometric diffusion neural processes

- Aim: probabilistic model over features fields.
- Constructed diffusion models over function space by correlating finite marginals
- Incorporating group invariance by
  - targetting invariant Gaussian processes and
  - parameterising the score with an equivariant neural network
- Sampling from the conditional process with Langevin corrector
- Empirically demonstrated modelling capacity on scalar and vector fields, with Euclidean and spherical output space

Thank you for your attention. Questions?

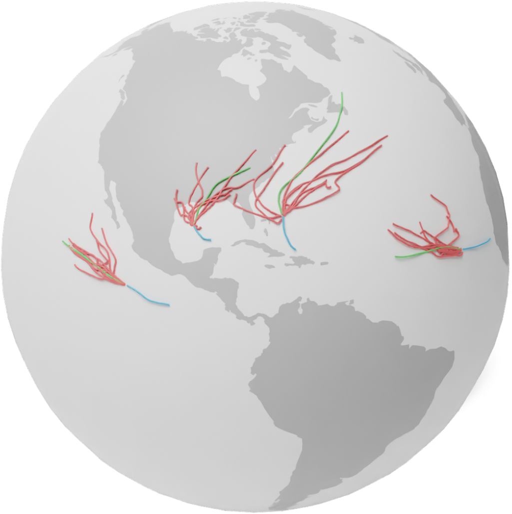

Credits to Michael Hutchinson for this 3D render.

Appendix

Steerable feature fields

A **feature field** is a tuple (f, ρ) with $f : \mathcal{X} \rightarrow \mathbb{R}^d$ a mapping between $x \in \mathcal{X}$ to some feature $f(x)$ with representation $\rho : G \rightarrow \mathrm{GL}(\mathbb{R}^d)$ (Scott and Serre, 1996).
The action of $G = \mathrm{E}(d) = \mathrm{T}(d) \rtimes \mathrm{O}(d)$ on the feature field f given by

$$g \cdot f(x) = (uh) \cdot f(x) \triangleq \rho(h) f\left(h^{-1}(x-u)\right) \tag{9}$$

Typical examples of feature fields include:

- **Scalar fields** $\rho_{\mathrm{triv}}(h) \triangleq 1$ e.g. temperature or potential fields.
- **Vectors fields** $\rho_{\mathrm{Id}}(h) \triangleq h$ e.g. wind or force fields.

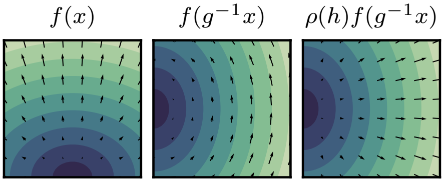

1D regression: Kernel ablation

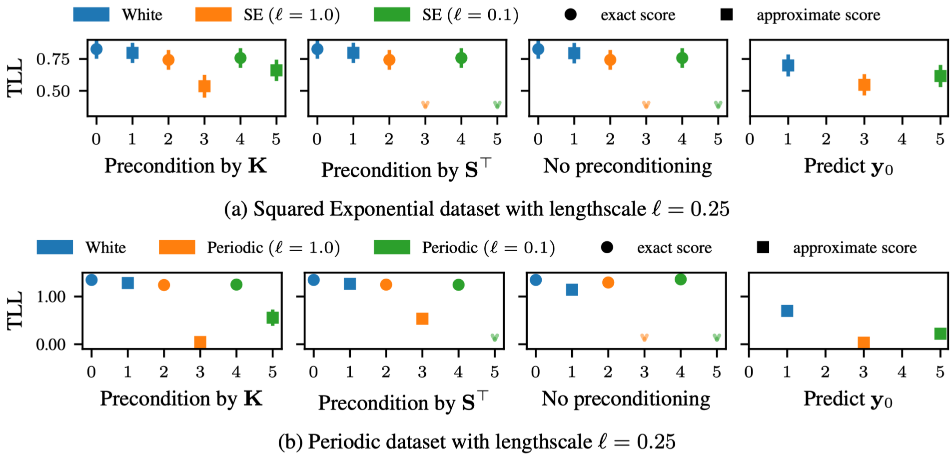

Figure 14: Ablation study targeting different limiting kernels and score parametrisations.

References

M. S. Albergo and E. Vanden-Eijnden. Building Normalizing Flows with Stochastic Interpolants. Oct. 2022. DOI: 10.48550/arXiv.2209.15571. Cited on page 7.

V. D. Bortoli, E. Mathieu, M. J. Hutchinson, J. Thornton, Y. W. Teh, and A. Doucet. Riemannian Score-Based Generative Modelling. In *Thirty-Sixth Conference on Neural Information Processing Systems*, 2022. Cited on page 60.

W. Bruinsma, J. Requeima, A. Y. K. Foong, J. Gordon, and R. E. Turner. Gaussian Neural Processes. In *3rd Symposium on Advances in Approximate Bayesian Inference*, Feb. 2020. Cited on page 57.

P. Cattiaux, G. Conforti, I. Gentil, and C. Léonard. Time reversal of diffusion processes under a finite entropy condition. *arXiv preprint arXiv:2104.07708*, 2021. Cited on pages 14, 15.

P. Dhariwal and A. Nichol. Diffusion Models Beat GANs on Image Synthesis. 2021. arXiv: 2105.05233 [cs.LG]. Cited on pages 50, 51.

M. A. Finzi, A. Boral, A. G. Wilson, F. Sha, and L. Zepeda-Núñez. User-defined Event Sampling and Uncertainty Quantification in Diffusion Models for Physical Dynamical Systems. In *International Conference on Machine Learning*, pages 10136–10152. PMLR, 2023. Cited on pages 50, 51.

U. G. Haussmann and E. Pardoux. Time reversal of diffusions. *The Annals of Probability*, 14(4):1188–1205, 1986. Cited on pages 14, 15.

P. Holderrieth, M. J. Hutchinson, and Y. W. Teh. Equivariant Learning of Stochastic Fields: Gaussian Processes and Steerable Conditional Neural Processes. In *International Conference on Machine Learning*, 2021. Cited on pages 41, 42.

A. Hyvärinen. Estimation of non-normalized statistical models by score matching. *Journal of Machine Learning Research*, 6(4), 2005. Cited on page 16.

H. J. Knapp Kenneth R. Diamond, J. P. Kossin, M. C. Kruk, and C. J. I. Schreck. International Best Track Archive for Climate Stewardship (IBTrACS) Project, Version 4. Technical report, NOAA National Centers for Environmental Information, 2018. DOI: `https://doi.org/10.25921/82ty-9e16`. Cited on page 60.

A. Lugmayr, M. Danelljan, A. Romero, F. Yu, R. Timofte, and L. Van Gool. Repaint: Inpainting using denoising diffusion probabilistic models. In *Proceedings of the IEEE/CVF Conference on Computer Vision and Pattern Recognition*, pages 11461–11471, 2022. Cited on pages 50, 51.

I. Macêdo and R. Castro. *Learning Divergence-Free and Curl-Free Vector Fields with Matrix-Valued Kernels*. Pré-Publicações / A.: Pré-publicações. IMPA, 2010. Cited on pages 41, 42.

A. Phillips, T. Seror, M. Hutchinson, V. De Bortoli, A. Doucet, and E. Mathieu. Spectral Diffusion Processes. Nov. 2022. URL: http://arxiv.org/abs/2209.14125. Cited on pages 30–32.

A. Ramesh, P. Dhariwal, A. Nichol, C. Chu, and M. Chen. Hierarchical Text-Conditional Image Generation with CLIP Latents. Apr. 2022. DOI: 10.48550/arXiv.2204.06125. Cited on pages 50, 51.

S. Ravuri, K. Lenc, M. Willson, D. Kangin, R. Lam, P. Mirowski, M. Fitzsimons, M. Athanassiadou, S. Kashem, S. Madge, R. Prudden, A. Mandhane, A. Clark, A. Brock, K. Simonyan, R. Hadsell, N. Robinson, E. Clancy, A. Arribas, and

S. Mohamed. Skilful Precipitation Nowcasting Using Deep Generative Models of Radar. *Nature*, 597(7878):672–677, Sept. 2021. ISSN: 0028-0836, 1476-4687. DOI: 10.1038/s41586-021-03854-z. Cited on page 5.

L. Scott and J. Serre. *Linear Representations of Finite Groups*. Graduate Texts in Mathematics. Springer New York, 1996. ISBN: 978-0-387-90190-9. URL: https://books.google.co.uk/books?id=NCfZgr54TJ4C. Cited on page 65.

Y. Song, J. Sohl-Dickstein, D. P. Kingma, A. Kumar, S. Ermon, and B. Poole. Score-Based Generative Modeling through Stochastic Differential Equations. In *International Conference on Learning Representations*, 2021. Cited on pages 9, 16.

B. L. Trippe, J. Yim, D. Tischer, T. Broderick, D. Baker, R. Barzilay, and T. Jaakkola. Diffusion Probabilistic Modeling of Protein Backbones in 3D for the Motif-Scaffolding Problem. June 2022. DOI: 10.48550/arXiv.2206.04119. Cited on pages 4, 50, 51.

P. Vincent. A connection between score matching and denoising autoencoders. *Neural Computation*, 23(7):1661–1674, 2011. Cited on page 16.

M. Xu, L. Yu, Y. Song, C. Shi, S. Ermon, and J. Tang. GeoDiff: A Geometric Diffusion Model for Molecular Conformation Generation. In *International Conference on Learning Representations*, 2022. URL: https://openreview.net/forum?id=PzcvxEMzvQC. Cited on page 4.